

**Electro Magneto-Hydrodynamic Peristaltic
Transport of Dusty Fluid**



By

MUHAMMAD LUQMAN

283-FBAS/MSMA/F15

Supervised by

Dr. AHMED ZEESHAN

**Department of Mathematics and Statistics
Faculty of Basic and Applied Sciences
INTERNATIONAL ISLAMIC UNIVERSITY,
ISLAMABAD, PAKISTAN
2017**

MS
532
LUE

Fluid mechanics.
" dynamics.
Mathematical formulation

MS
532
LUE

Fluid mechanics.
" dynamics.
Mathematical formulation

**Electro Magneto-Hydrodynamic Peristaltic
Transport of Dusty Fluid**



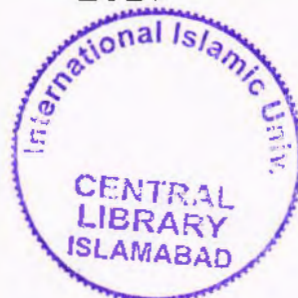
By

MUHAMMAD LUQMAN

283-FBAS/MSMA/F15

**Department of Mathematics and Statistics
Faculty of Basic and Applied Sciences
INTERNATIONAL ISLAMIC UNIVERSITY,
ISLAMABAD, PAKISTAN**

2017



**Electro Magneto-Hydrodynamic Peristaltic
Transport of Dusty Fluid**

By

MUHAMMAD LUQMAN

A Dissertation

Submitted in the Partial Fulfillment of the

Requirements for the Degree of

MASTER OF SCIENCE

In

MATHEMATICS

Supervised by

Dr. AHMED ZEESHAN

**Department of Mathematics and Statistics
Faculty of Basic and Applied Sciences
INTERNATIONAL ISLAMIC UNIVERSITY,
ISLAMABAD, PAKISTAN
2017**

Certificate

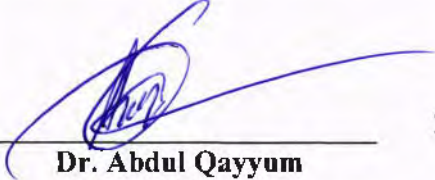
Electro magnetohydrodynamics peristaltic transport of dusty fluid

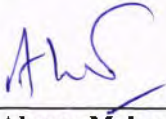
By

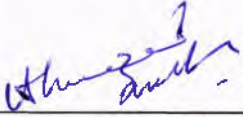
Muhammad Luqman

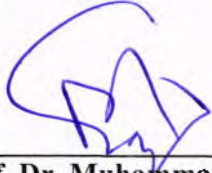
A DISSERTATION SUBMITTED IN THE PARTIAL FULFILLMENT OF THE REQUIREMENTS
FOR THE DEGREE OF THE MASTER OF SCIENCE IN MATHEMATICS

We accept this dissertation as conforming to the required standard.

1. 

Dr. Abdul Qayyum
External Examiner
2. 

Dr. Ahmer Mehmood
Internal Examiner
3. 

Dr. Ahmed Zeeshan
Supervisor
4. 

Prof. Dr. Muhammad Sajid, T.I
Chairman

**Department of Mathematics & Statistics
Faculty of Basic and Applied Sciences
International Islamic University, Islamabad
Pakistan
2017**

Declaration

The work described in this thesis is carried out under the supervision and guidance of Dr. Ahmed Zeeshan Department of Mathematics and Statistics, International Islamic University, Islamabad. No portion of this work referred in this thesis is submitted in support of another degree or qualification either in this university or any other institute. This thesis is my original work except where due references are given.

Signature: _____
Muhammad Luqman
MS (Mathematics)

**Dedicated to
My Family
&
Teachers.**

Acknowledgements

First of all, I am thankful to everlasting **Allah**, the creator of mankind who granted us health, knowledge and intelligence to extract the hidden realities in the universe through scientific and critical approach. I pay my special thanks to almighty **Allah** who provide me the strength and ability to learn and to achieve another milestone to a destination. Countless daroods and Salams upon **Prophet Hazrat Muhammad (SAW)** who has lightened the life of mankind with his guidance.

Foremost thanks go to my supervisor **Dr. Ahmed Zeeshan**, for his regardless and inspirational efforts and moral support throughout my research carrier. His comprehensive knowledge and logical way of thinking have been of greater value for me. May **Allah** bless him with all kinds of happiness and success in life and may his all wishes come true.

This dissertation is dedicated to my late father who has been my constant source of inspiration. I am also most grateful to my mother and family for their belief in me and their constant prayers and kind support.

I owe my deepest gratitude to Prof. Dr. Muhammad Sajid, the head of Mathematics department, for his motivation and immense knowledge.

Many thanks to Dr. Rahmat Ellahi, Dr. Tariq Javid, Dr. Nasir Ali and Dr. Ahmer Mehmood for their valuable discussions that helped me to understand my research in a better way. They always directed me to the right dimensions and made it possible for me to achieve an attractive goal.

A warm thanks to Mr. Muddassar Maskeen, Mr. Nasir Shehzad, Mr. Noman Ijaz, Mr. Aqib Majeed, Mr. Farooq Hussain and MS fellows for their intellectual support, love, care and entertainment they provided.

Muhammad Luqman

Contents

1 Preliminaries	
1.1 Fluid Mechanics	1
1.2 Branches of Fluid Mechanics	1
1.2.1 Fluid statics	1
1.2.2 Fluid kinematics	1
1.2.3 Fluid dynamics	1
1.3 Fluid	1
1.4 Flow	2
1.5 Types of flow	2
1.5.1 Uniform flow	2
1.5.2 Non uniform flow	2
1.5.3 Laminar flow	2
1.5.4 Turbulent flow	2
1.5.5 Steady and Un-steady flow	3
1.5.6 Compressible and incompressible flow	3
1.5.7 Ideal and real flow	3
1.5.8 Internal and external flow	3
1.6 Properties of fluid	4
1.6.1 Viscosity	4
1.6.2 Density	4
1.6.3 Pressure	5
1.6.4 Stress	5
1.6.5 Shear stress	6
1.6.6 Normal stress	6
1.6.7 Strain	6
1.7 Dimensionless numbers	6
1.7.1 Reynolds number	6
1.7.2 Hartmann number	7
1.7.3 Helmholtz-Smoluchowski	7
1.7.4 Electro-osmotic	8
1.8 Magneto hydrodynamic	8
1.9 Electro hydrodynamic	9
1.10 Peristalsis	9
2 Transverse magnetic field driven modification in unsteady peristaltic transport with electrical double layer effects	
2.1 Mathematical formulation	12
2.2 Numerical results and discussion.	17
2.2.1 Axial velocity	17
2.2.2 Pressure distribution.	17
2.2.3 Local wall shear stress	18
2.2.4 Averaged volumetric flow rate	18
2.2.5 Streamlines.	19

2.3	Concluding remarks	25
3	Electro magneto-hydrodynamic peristaltic transport of dusty fluid	
3.1	Mathematical formulation	26
	3.1.1 Fluid phase	26
	3.1.2 Particulate phase	27
3.2	Solution of the problem	28
3.3	Numerical result and discussion	30
	3.3.1 Fluid and Particle velocity profile	30
	3.3.2 Pressure gradient	31
	3.3.3 Skin friction	31
	3.3.4 Stream lines	31
3.4	Concluding remarks	44
4	References	45

Preface

The technological advances have been made in the field of micro scale pumping designs including the development of microfluidics devices, micro pumping and peristaltic micro pumping [2]. An electro-osmotic pump is capable of generating high pressure and flow without moving mechanical parts and a robust design in this regard has been presented by Goodson *et al.* at the Nano Heat Mechanical Engineering Laboratory, Stanford University, USA [3]. Peristalsis is a physiological mechanism which achieves excellent and efficient transport of materials via periodic contraction of the conveying conduit. In this sense it is a *smart system* as it responds to electrical nerve stimulation and is mobilized intelligently to varying needs. Exploiting this principle of peristalsis, an electrostatically-actuated, biomimetic, micro- peristaltic pump has also been designed [3-8].

As elaborated earlier, peristalsis is a unique mechanism in biology which comprises an automatic periodic series of muscle contractions and relaxation that occurs during movement of, for example, food bolus through the digestive system, urine flow from the kidneys into the bladder, transportation of bile from the gall bladder into the duodenum and many other physiological systems. Peristalsis has been studied in medical sciences for over a century. In the context of theoretical and experimental fluid dynamics, it received attention in the mid-1960s onwards, again motivated by the development of efficient pumps for medical and other applications. Important mathematical works in this regard have been communicated [9-16] include Tripathi and Bég [17-18] and also Blanchette [19] and Ellahi *et al.* [20] who computed heat transfer in peristaltic flow. Further recent studies exploring other areas of peristaltic transport are the articles of Tripathi and Bég [21].

This dissertation is divided into three chapters. Chapter 1 contains the definition and basic concepts related to peristalsis. In chapter 2, the study of transverse magnetic field driven modification in

unsteady peristaltic transport with electrical double layer effects is discussed [1]. The effects of a transverse magnetic field on time-dependent peristaltic transport of electrically-conducting fluids through a micro channel under an applied external electric field with induced electric field effect is considered, based on lubrication theory approximations. The flow problem is modelled using continuity and Navier-Stokes equations. The long wavelength and low Reynolds number approximation is used to simplify the equations. The analytic solution of the equations are derived. The impact of parameters such as Hartmann number, electro-osmotic have been observed graphically. Whereas chapter 3 is discussed Electro magneto-hydrodynamic peristaltic transport of dusty fluid. The flow is described by law of conservation of mass and momentum. The fluid is assumed to be incompressible. The solution is obtained numerically. The effects of parameters are plotted.

Chapter 1

1 Preliminaries

In this chapter some basic definitions and parameters are defined, which are helpful in the subsequent chapters.

1.1 Fluid Mechanics

Fluid mechanics is the branch of physics which involves the study of fluids (liquids, gas, and plasmas) and the forces on them.

1.2 Branches of fluid mechanics

1.2.1 Fluid statics

It is the study of fluid at rest. For example, the study of water at sea or the study of oil in gallon.

1.2.2 Fluid kinematics

The study of fluids which are in motion. For example, the study of water in river or the study of oil in pipe.

1.2.3 Fluid dynamics

The study of the effect of forces on the fluid motion. It is the branch of continuum mechanics which deals with the properties of stationary and moving fluids.

1.3 Fluid

A fluid is a substance that deforms continuously when subjected to a shear stress, no matter how small that shear stress may be. In simple words, a fluid is a substance which is capable of flowing and which conforms to the shape of containing vessel.

1.4 Flow

A material goes under deformation when different forces act on it. If deformation increases continuously without any limit then the phenomenon is known as flow.

1.5 Types of flow

1.5.1 Uniform flow

A flow in which fluid particles possess with the same velocity at each section of a channel or a pipe is called uniform flow.

1.5.2 Non-uniform flow

A flow in which fluid particles possess through different velocities at each section of a channel or a pipe is called non-uniform flow.

1.5.3 Laminar flow

A flow in which each particle has a definite path and the path of individual particles does not cross each other is called laminar flow.

1.5.4 Turbulent flow

Turbulent flow is a type of fluid (gas or liquid) flow in which the fluid undergoes irregular fluctuations, or mixing, in contrast to laminar flow, in which the fluid moves in smooth paths or layers. In turbulent flow the speed of the fluid at a point is continuously undergoing changes in both magnitude and direction.

1.5.5 Steady flow and Unsteady flow

A flow in which properties associated with the motion of fluid are independent of time or flow pattern and remains unchanged with the time is a called steady flow. Mathematically it can be defined as:

$$\frac{\partial V}{\partial t} = 0,$$

All those flows in which properties associated with the motion of fluid depend on time so that flow pattern vary with the time is called unsteady flow. Flow in ocean tides is an example of unsteady flow. Mathematically is narrated as:

$$\frac{\partial V}{\partial t} \neq 0.$$

1.5.6 Incompressible and compressible flows

The flow of an incompressible fluid (i.e. for which the density remains constant throughout the fluid) is said to be incompressible flow. On the other hand, the flow of a compressible fluid i.e. for which the density is not constant is called a compressible flow.

1.5.7 Ideal and real flows

The flow of an ideal (i.e. in viscid and incompressible) fluid is said to be ideal flow, while the flow of a real (i.e. viscous) fluid is called a real flow.

1.5.8 Internal and external flows

Internal flows are those where fluid flow through confined spaces such as pipes, open channel, and fluid mechanics. The internal flow of liquids in which the channel does not flow full is called an

open channel flow. For example, flow in rivers and irrigation canals. External flows occur over bodies immersed in an unbounded fluid, such as atmosphere through which airplanes, missiles, and space vehicle travel, or the ocean water through which submarines and torpedoes.

1.6 Properties of fluids

1.6.1 Viscosity

It is the measure of internal resistance of a fluid to flow or it may be thought of a measure of fluid friction. In other words, it is defined as the ratio of shear stress to the rate of shear strain.

Mathematically it can be expressed as shear stress

$$\mu = \frac{\text{shear stress}}{\text{rate of shear strain}},$$

where, μ is called dynamic viscosity. Its unit is pa. s. For example, pushing a spoon with a small force moves it easily through a bowl of water, but the same force moves mashed potatoes very slowly.

1.6.2 Density

Density of a fluid is defined as mass per unit volume. Mathematically, density ρ at a point P may be defined as

$$\rho = \lim_{\delta v \rightarrow 0} \frac{\delta m}{\delta v},$$

where, δv is total volume element around the point and δm is the mass of fluid.

1.6.3 Pressure

Pressure is defined as force per unit area. It is usually more convenient to use pressure rather than force to describe the influences upon fluid behavior. The standard unit for Pressure is the Pascal, which is a Newton per square meter. Mathematically,

$$P = \frac{F}{A}.$$

The SI derived unit of pressure is Pascal (symbol: Pa) or $\frac{N}{m^2}$.

1.6.4 Stress

The stress or stress vector is defined as the force per unit area of the force on which it acts. If the stress is uniformly distributed over the plan area A , the stress called the average stress is defined

as $\frac{\vec{F}}{A}$. The stress at any point P in the fluid is defined as

$$\text{Stress any point } P = \lim_{\Delta S \rightarrow 0} \frac{\Delta \vec{F}}{\Delta S},$$

where $\Delta \vec{F}$ is the force acting on an element of surface area ΔS enclosing the point P .

$$\sigma = \frac{F}{A},$$

where σ is stress (in Newton's per square meter or, equivalently, Pascal)

1.6.5 Shear stress

The shear stress, denoted by “ τ ” is defined as the component of stress coplanar with a material cross section. Shear stress arises from the force vector component parallel to the cross section.

Mathematically,

$$\tau = \lim_{\Delta A \rightarrow 0} \frac{\Delta F_t}{\Delta A}.$$

1.6.6 Normal Stress

Normal stress arises from the force vector component perpendicular to the material cross section on which it acts. Mathematically,

$$\sigma = \lim_{\Delta A \rightarrow 0} \frac{\Delta F_n}{\Delta A}.$$

1.6.7 Strain

The strain is the measure of how much deformation has occurred in the body compared its general shape due to the action of force.

1.7 Dimensionless numbers

1.7.1 Reynolds number

The ratio of inertial force to viscous force is said to be Reynolds number. Mathematically,

$$Re = \frac{\text{Inertial force}}{\text{Viscous force}}$$

1.7.2 Hartmann number

Hartmann number (Ha) is the ratio of electromagnetic force to the viscous force first introduced by Hartmann. It is defined by:

$$Ha = B_0 a \sqrt{\frac{\sigma}{\mu}}$$

where

- B is the magnetic field
- a is the characteristic length scale
- σ is the electrical conductivity
- μ is the dynamic viscosity

1.7.3 Helmholtz-Smoluchowski

$$U_{HS} = -\frac{E_{\xi} \epsilon \zeta}{\mu c}$$

- E_{ξ} is axially-applied electric field.
- ϵ is the permittivity.
- ζ is the zeta potential.
- μ is the dynamic viscosity
- c is the wave velocity.

1.7.4 Electro-osmotic

Electro-osmotic parameter is known as:

$$m = aez \sqrt{\frac{2n_0}{\epsilon K_B T}}$$

- a is the radius of tube.
- e is the electronic charge.
- z is the charge balance.
- n_0 is the concentration of ions at the bulk.
- ϵ is the permittivity.
- K_B is the Boltzmann constant.
- T is the Temperature.

1.8 Magneto hydrodynamic

Magneto hydrodynamics (MHD; also magneto-fluid dynamics or hydro magnetics) is the study of the magnetic properties of electrically conducting fluids. Examples of such magneto fluids include plasmas, liquid metals, salt water and electrolytes. The word "magneto hydrodynamics" is derived from *magneto-* meaning magnetic field, *hydro-* meaning water, and *-dynamics* meaning movement

1.9 Electro hydrodynamic

Electro hydrodynamics (EHD), also known as electro-fluid-dynamics (EFD) or electro kinetics, is the study of the dynamics of electrically charged fluids. It is the study of the motions of ionized particles or molecules and their interactions with electric fields and the surrounding fluid. The term may be considered to be synonymous with the rather elaborate electrostrictive hydrodynamics. ESHD covers the following types of particle and fluid transport mechanisms: electrophoresis, electro kinesis, electrophoresis, electro-osmosis, and electro rotation. In general, the phenomena relate to the direct conversion of electrical energy into kinetic energy, and *vice versa*.

1.10 Peristalsis

Peristalsis is an involuntary pattern of smooth muscle contractions mostly dealing in the process of digesting but also found in other hollow tubes of the body. It constitutes the wavelike contractions and relaxation of muscle. These waves can have short or long wavelength which moves through the whole length of the organ. The examples of such waves can be observed in urine transport from kidney, motion of food through digestive system and some blood vessels. Peristaltic wave are formed from through two major reflexes within body which are initiated by a bolus of food. These sensory neurons with two sets of interneuron's lead to two distinct effects. First of interneuron's activates excitatory motor neurons above the bolus contraction of smooth muscle above the bolus. Other interneurons activate inhibitory motor neurons that stimulate relaxation of smooth muscle below the bolus.

The word peristaltic originates from a Greek word "Peristaltic" which means clasping and compressing. Peristaltic pumping is a form of fluid transport generated in the fluid contained in a distensible tube when a progressive wave travels along the wall of the tube. It is an inherent property of much syncytial smooth muscle tube, stimulation at any point can cause a contractile ring to appear in the circular muscle of the gut and this ring then spreads along the tube. In such a way, peristaltic occurs in the gastrointestinal tract, the bile ducts, and other glandular ducts throughout the body, the ureters and many other smooth muscle tubes of the body.

The peculiar worm like wave motion of the intestines and other hollow muscular structures, produced by progressive contraction of the muscular fibers of their walls, forcing their contents onward is called peristaltic motion.

Physiological fluids in animal and human bodies are in general pumped by continuous periodic muscular oscillation of the ducts. These oscillations are presumed to be caused by the progressive transverse contraction waves that propagate along the walls of the ducts. Peristalsis is the mechanism of the fluid transport that occur generally from a region of lower pressure to higher pressure when a progressive wave of area contraction and expansion travels along the flexible wall of the tube. Peristaltic flow occur widely in the functioning of ureter, food mixing and chime movement in the intestine, movement of eggs in the fallopian tube, transport of the bile in the bile duct, transport of cilia and circulation of blood in small blood vessels. There are many important applications of this principle such as the design of roller pumps, which are useful in pumping fluid without contamination due to contact with pumping machinery.

Peristaltic is a form of fluid transport that occurs when a progressive wave of area contraction or expansion propagates along the length of distensible duct. Peristaltic is an inherent property of many biological systems having smooth muscle tubes which transports bio fluids by

its propulsive movements and is found in the transport of urine from the kidney to the bladder, the movement of chyme in the gastro-intestinal tract, intra-uterine fluid motion, vasomotion of the small blood vessels and in many other glandular ducts. Though the actual mechanism for the transport of water from the ground to upper branches of tall trees is not well understood, it is speculated that peristalsis and free convection contribute this motion. The diameters of the trunks of the trees are found to vary with time.

Peristaltic pumping by an infinite train of sinusoidal wave in the wall of two-dimensional tube is investigated theoretically when the inertial and streamline-curvature effects are moderate but not negligible as it is the case for roller pumps and the gastrointestinal tract. It is found that the pumping performance increases with increasing wall curvature and is decreased by inertial effects except at high squeeze. As in the inertia-free, infinite wavelength case there is a backward flow (reflux) near the moving walls which is enhanced by both the inertial and curvature effects. Under certain conditions, there are boluses of fluid moving at the wave speed as if they were trapped by the wave. The range of this trapping is decreased by inertial effects and increased by curvature effects.

Chapter 2

Transverse magnetic field driven modification in unsteady peristaltic transport with electrical double layer effects

In this chapter the work of Beg et al. [1] is revisited. All the equations and results are reproduced and presented. Here, the effects of electrical double layer on unsteady peristaltic transport of Newtonian fluid in the presence of magnetic field is modeled. The fluid is induced due to peristaltic work on flexible walls. The problem is modeled using law of conservation of mass and momentum. The dimensional parameter with assumption that $Re \rightarrow 0$ and $\delta \rightarrow \infty$ is used to reduce the equation, exact solution is obtained. Mathematica is used to draw the graphs to see the effects of parameters.

2.1 Mathematical formulation:

Under the transverse magnetic field, the geometry of model of electro kinetic peristaltic transport of a fluid through a channel of finite length (L), with electromagnetic biomimetic pump, shown in Fig.2.1. The wave on the wall mathematically represented by:

$$\bar{h}(\bar{\xi}, \bar{t}) = \left. \begin{array}{l} a - \bar{\phi} \cos^2 \frac{\pi}{\lambda} (\bar{\xi} - c\bar{t}), \text{ if } t < \xi < t+1 \\ a - \bar{\phi}, \text{ if } \xi \in [0, t] \cup [t+1, L] \end{array} \right\}, \quad (2.1)$$

Where, L , \bar{t} , c , $\bar{\xi}$, λ , $\bar{\phi}$, a , the channel length, time, wave velocity, axial coordinate, wavelength, amplitude and radius of channel.

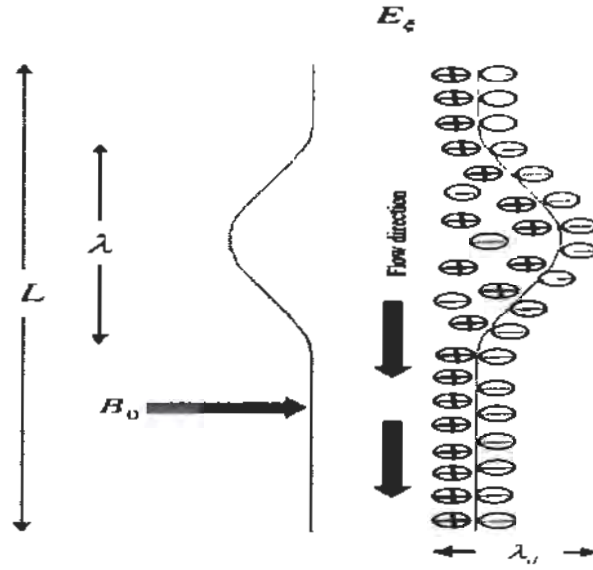


Fig.2.1 Model of problem

The governing equations for incompressible, unsteady flow by applying an electro kinetic force in the static magnetic field in the transverse and axial direction can be presented as:

$$\bar{\nabla} \cdot \bar{V} = 0, \quad (2.2)$$

$$\rho \left\{ \frac{\partial \bar{V}}{\partial t} + (\bar{V} \cdot \bar{\nabla}) \bar{V} \right\} = -\bar{\nabla} p + \mu \bar{\nabla}^2 \bar{V} + \bar{\rho}_e \bar{V} + \bar{J} \times \bar{B}, \quad (2.3)$$

where \bar{E} , μ , \bar{p} , \bar{V} , ρ , and $\bar{\rho}_e$ denote the electro kinetic body force, fluid viscosity, pressure, velocity vector, fluid density and charge density respectively, here due to ohm's law $\bar{J} = \sigma(\bar{E} + \bar{V} \times \bar{B})$ is the current density, σ is fluid electrical conductivity and \bar{B} is magnetic field.

The Poisson-Boltzmann equation for the electric potential distribution is described as:

$$\nabla^2 \bar{\phi} = -\frac{\bar{\rho}_e}{\epsilon}, \quad (2.4)$$

Where, ϵ is the permittivity and $\rho_e = ez(n^+ - n^-)$ in which n^+ and n^- are the number of densities of cation and anions respectively, by Boltzmann distribution given. $n^\pm = n_0 \text{Exp} \left[\mp \frac{ez\bar{\phi}}{K_B T} \right]$, where n_0 denotes the concentration of ions, z is charge balance, e is electronic charge, K_B is Boltzmann constant, T is the average temperature. Introducing a potential function $\bar{\phi}$ along the zeta potential ζ the non-dimensional variables like $\phi = \frac{\bar{\phi}}{\zeta}$, is obtained assuming,

$$\text{Sinh} \left(\frac{ez\bar{\phi}}{K_B T} \right) \approx \frac{ez\bar{\phi}}{K_B T} \text{ and applying the boundary conditions } \left. \frac{\partial \phi}{\partial \eta} \right|_{\eta=0} = 0 \text{ and } \phi|_{\eta=h} = 1.$$

The potential function is:

$$\phi = \frac{\text{Cosh}(m\eta)}{\text{Cosh}(mh)}, \quad (2.5)$$

Where $m = aez \sqrt{\frac{2n_0}{\epsilon K_B T}} = \frac{a}{\lambda_d}$, recognized as electro-osmotic parameter, $\lambda_d = \frac{1}{m}$ is the Debye length. The electro magneto-hydrodynamic peristaltic transport of fluid is overseen equations under review of low Reynolds number and long wave length.

$$\frac{\partial u}{\partial \xi} + \frac{\partial v}{\partial \eta} = 0, \quad (2.6)$$

$$\frac{\partial p}{\partial \xi} = \frac{\partial^2 u}{\partial \eta^2} - Ha^2 u - m^2 U_{HS} \Phi, \quad (2.7)$$

where ξ , η , u , v the axial coordinate, transverse are coordinate, axial velocity and the transverse velocity. $Ha = B_0 a \sqrt{\frac{\sigma}{\mu}}$ is Hartmann number, $Re = \frac{\rho c a}{\mu}$ is the Reynolds number, $U_{HS} = -\frac{E_\xi \epsilon \zeta}{\mu c}$

is the Helmholtz-Smoluchowski velocity and E_ξ is the axially applied electric field. So the boundary conditions are:

$$\left. \frac{\partial u}{\partial \eta} \right|_{\eta=0} = 0, u|_{\eta=h} = 0, v|_{\eta=0} = 0, v|_{\eta=h} = \frac{\partial h}{\partial t}, p|_{\xi=0} = p_0 \text{ and } p|_{\xi=L} = p_L. \quad (2.8)$$

The axial velocity is gained, by integrating Eq. (2.7) along with boundary conditions in Eq. (2.8)

$$u = \frac{1}{Ha^2} \frac{\partial p}{\partial \xi} \left\{ \frac{\cosh(Ha\eta)}{\cosh(Hah)} - 1 \right\} + \frac{m^2 U_{HS}}{m^2 - Ha^2} \left\{ \frac{\cosh(m\eta)}{\cosh(mh)} \frac{\cosh(Ha\eta)}{\cosh(Hah)} \right\}. \quad (2.9)$$

From the Equation of continuity, we get transverse velocity by using Eq. (2.9) and boundary conditions (2.8)

$$v = -\frac{1}{Ha^2} \left\{ \frac{\partial^2 p}{\partial \xi^2} \left(\frac{\sinh(Ha\eta)}{Ha \cosh(Hah)} - \eta \right) + \frac{\partial p}{\partial \xi} \frac{\partial h}{\partial \xi} \frac{\sinh(Hah) \tanh(Hah)}{\cosh(Hah)} \right\} + \frac{m^2 U_{HS}}{m^2 - Ha^2} \left\{ \frac{\sinh(Ha\eta) \tanh(Hah)}{\cosh(Hah)} - \frac{\sinh(m\eta) \tanh(mh)}{\cosh(mh)} \right\} \frac{\partial h}{\partial \xi}, \quad (2.10)$$

and the pressure gradient appears, by using Eq. (2.10) and the boundary condition (2.8)

$$\frac{\partial p}{\partial \xi} = \frac{Ha^3}{Hah - \tanh(Hah)} \left[G_0(t) + \int \frac{\partial h}{\partial t} d\xi - \frac{m^2 U_{HS}}{m^2 - Ha^2} \left\{ \frac{\tanh(Ha\eta)}{Ha} - \frac{\tanh(m\eta)}{m} \right\} \right], \quad (2.11)$$

Where, $G_0(t)$ is the arbitrary time function can be evaluated using the finite length boundary conditions. The pressure can be obtained by using this expression

$$\Delta p = p(\xi, t) - p(0, t) = \int_0^\xi \frac{\partial p}{\partial s} ds \quad (2.12)$$

Now, $G_0(t)$ is defined as

$$G_0(t) = \frac{(P_t - P_0) - \int_0^L \frac{Ha^3}{Hah - \tanh(Hah)} \left[\int \frac{\partial h}{\partial t} d\xi - \frac{m^2 U_{HS}}{m^2 - Ha^2} \left\{ \frac{\tanh(Ha\eta)}{Ha} - \frac{\tanh(m\eta)}{m} \right\} \right] d\xi}{\int_0^L \frac{Ha^3}{Hah - \tanh(Hah)} d\xi} \quad (2.13)$$

The local wall shear stress is

$$\tau_w = \frac{\partial u}{\partial \eta} \Big|_{\eta=h} = \frac{\tanh(Hah)}{Ha} \frac{\partial p}{\partial \xi} + \frac{m^2 U_{HS}}{m^2 - Ha^2} \{ m \tanh(mh) - Ha \tanh(Hah) \}. \quad (2.14)$$

The relation for flow rate is

$$Q(\xi, t) = \int_0^h u d\eta = \frac{1}{Ha^3} \frac{\partial p}{\partial \xi} \{ \tanh(Hah) - Hah \} + \frac{m^2 U_{HS}}{m^2 - Ha^2} \left\{ \frac{\tanh(mh)}{m} - \frac{\tanh(Hah)}{Ha} \right\}. \quad (2.15)$$

The average volumetric flow can be written as

$$\bar{Q} = \int_0^1 Q dt = Q + 1. \quad (2.16)$$

Using the equation (2.9), the stream function become

$$\psi = \frac{1}{Ha^2} \frac{\partial p}{\partial \xi} \left\{ \frac{\sinh(Ha\eta)}{Ha \cosh(Hah)} - \eta \right\} + \frac{m^2 U_{HS}}{m^2 - Ha^2} \left\{ \frac{\sinh(m\eta)}{m \cosh(mh)} - \frac{\sinh(Ha\eta)}{Ha \cosh(Hh)} \right\}. \quad (2.17)$$

2.2 Numerical results and discussion:

In given section graphical result of analytic relation are account variation of variety of parameters on velocity, pressure, shear stress and flow rate are shown from Fig (2.2-2.6).

2.2.1 Axial velocity:

Figs. (2.2 a-b) change in the axial velocity (u_0) against the Hartmann number (Ha), (a) electro-osmotic parameter (m), (b). U_{HS} max. Electro-osmotic velocity. Axial velocity is expressively increase by using the greater value of Hartmann number, as certified by decrease the values of

(u_0) in negative along the increasing Ha . $Ha = B_0 a \sqrt{\frac{\sigma}{\mu_s}}$ define relative effect of the magnetic

body force towards viscous force. Conversely, by increasing the values of electro-osmotic parameter m , there is deceleration in axial flow. The electrostatic body force $m^2 H_{HS} \phi$, so the flow in system, magnetic body force have opposite effect.

2.2.2 Pressure distribution:

Figs. (2.3 a-d) presents change in the pressure difference (Δp) the axial coordinate (ξ) and time (t) along with the variations in Hartmann numbers (Ha). The periodic nature flow can be clearly captured which is related with the peristaltic wave due to deformable channel walls. By raising the Hartmann number an important elevation the pressure difference in figs (2.3 a-d) at $t=0$, $t=0.3$, $t=0.6$ and 0.9 respectively. With evolution in time that have opposite effect computed i.e. pressure differences are repressed with increasing Hartmann number. So according to the real-time electromagnetic, Hartmann number whereas initially attaining an increase in hydrodynamic

pressure, along the more time elapse bases the different effect. Pressure differences are also establish to reduce with the higher axial distance (ξ).

2.2.3 Local wall shear stress:

Figs. (2.4 a-d), illustrate the shapes of local wall shear stress (τ_w) along the axial coordinate (ξ), Hartmann number (Ha) and time (t). At $t=0$, as shown in Fig (4a), initially in the wall shear stress through little change in the axial coordinate, variation in the wall shear stress is noticed for increasing the values of axial coordinate. In the wall shear stress the raise in the graph at a one location as of the inlet. With the variation of time in Figs. (4-b, c, d) dual peak observed with the dual change. The peak evacuated from the inlet by raising time. The time-dependent nature of peristaltic wave is revealed the step size changes in wall stress.

2.2.4 Averaged volumetric flow rate:

Figs. (2.5 a, b) show the graph averaged volumetric flow rate (\bar{Q}_0) with the variation of Hartmann number (Ha), electro-osmotic parameter (m) and the external electrical field parameter U_{ES} . Flow rate in Fig. (5a). is start reducing with the greater Hartmann number which is caused by the greater magnetic field. The opposite reaction is continued with greater electro-osmotic parameter. In the same way in Fig. (5b) raise in electrical field parameter that observe the maximum averaged flow rate. The magnitudes of the flow rates in the Figs. (5-a, b) are same.

2.2.5 Streamlines:

Figs. (2.6 a-d), shows the streamline using the variations of Hartmann number. In all variations of Hartmann number electrical field special effects exists ($U_{HS} = 1$ and $m = 5$). The visualization permits a well analysis of the trapping phenomenon, also a rotating bolus of fluid made a sealed form streamlines. For $Ha = 0.001$ i.e. in Fig. (2.6a) the magnetic body force is *weaker* than viscous body force. The result of viscosity in the demonstration of the twin system for different boluses enclosed with other regions of the trapped flow. The streamlines are adjacent and parallel to $\xi = 0$ lines are mainly accurate and these line defines the two different bolus zones. When $Ha = 1$ in Fig. (6b), magnetic force increases thousand fold and this helps to define the bolus zones. By increase the Hartmann number $Ha = 2$ in Fig.(2.6c), dual zones fail to maintain concentration of the streamlines near to each other, and bolus can be seen in the each zone. However, more raise in the Hartmann number $Ha = 3$ in the Fig. (2.6 d) there is presence of the streamlines about bolus and development of the different zones turn into intensified.

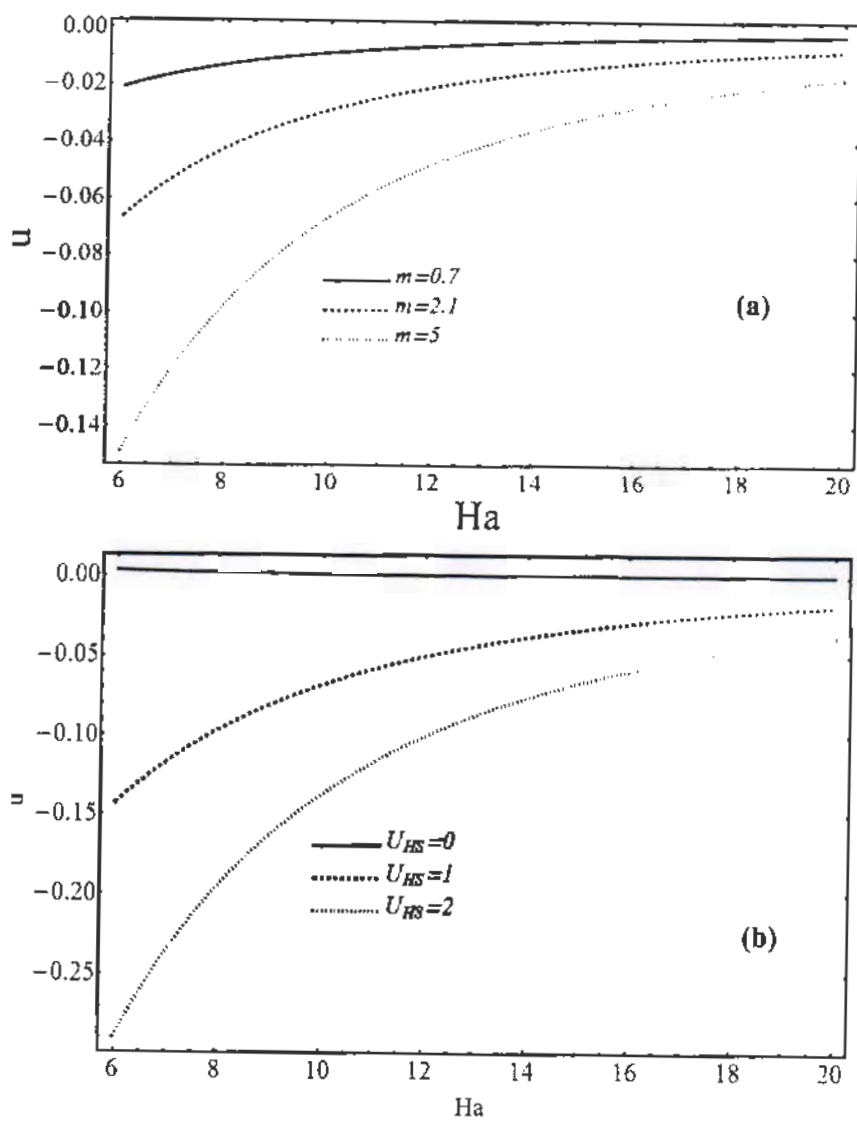


Fig.2.2 Axial velocity at $\varphi = 0.6$ (a) $U_{HS} = 1$ for the Debye length
 (b) $m = 5$ for the external electric field.

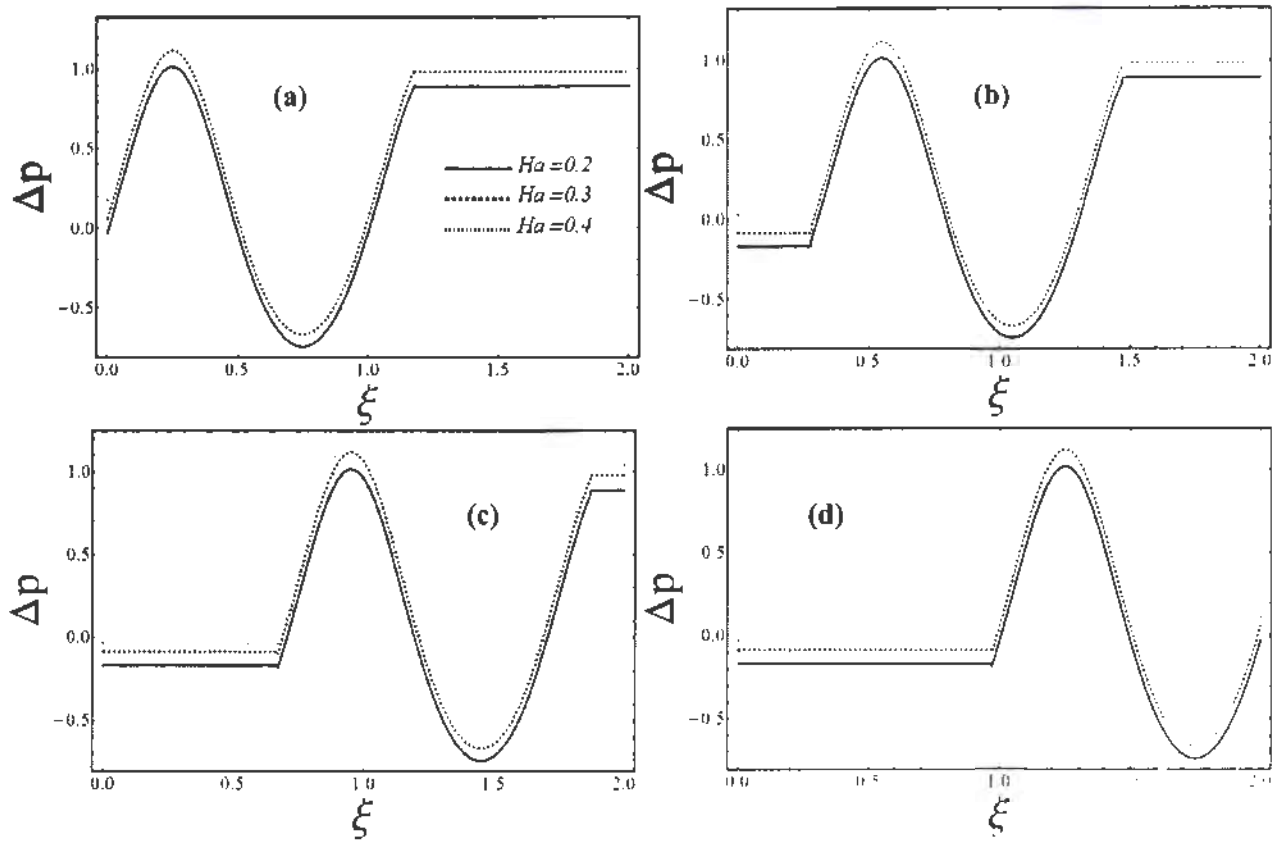


Fig.2.3 Pressure distribution for the different values of Hartmann number at
 (a) $t = 0$, (b) $t = 0.3$, (c) $t = 0.6$, (d) $t = 0.9$ when $\varphi = 0.6, l = 2, p_l = p_0 = 0, U_{HS} = 1, m = 5$

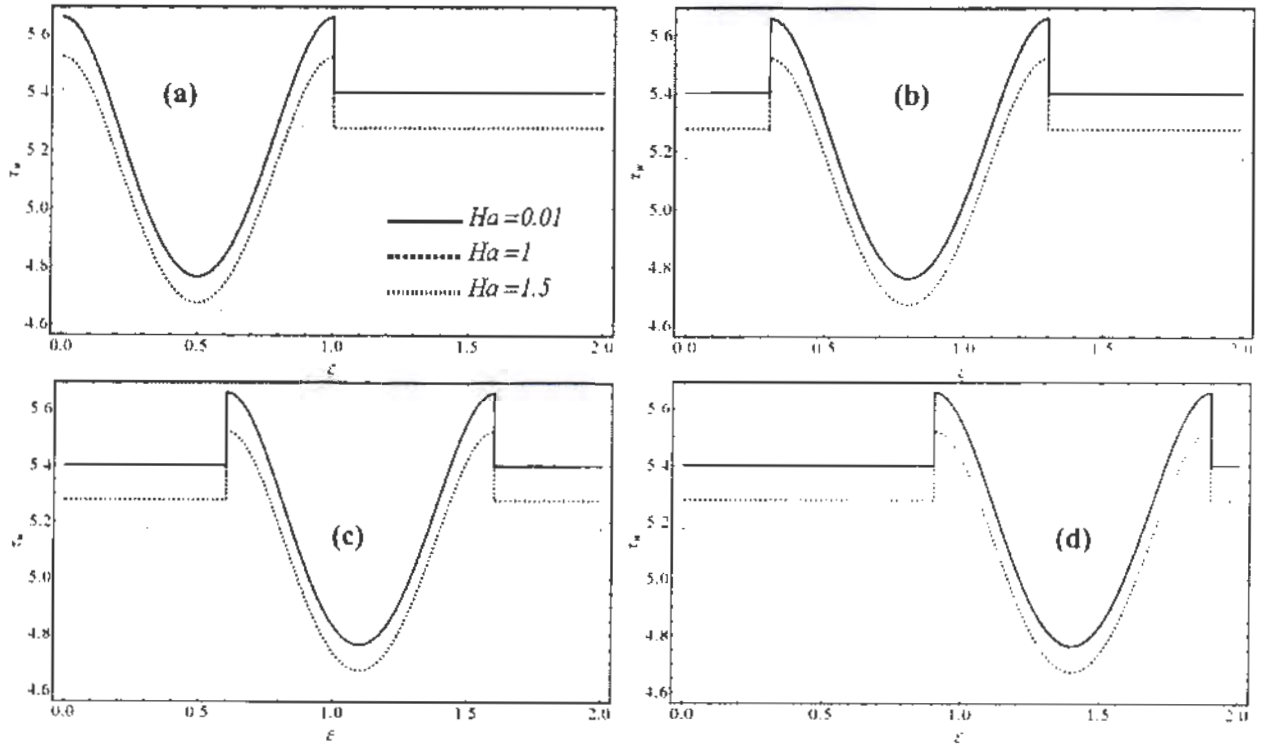


Fig.2.4 Local wall shear for the different values of Hartmann number

(a) $t = 0$, (b) $t = 0.3$, (c) $t = 0.6$, (d) $t = 0.9$ when $\varphi = 0.6, l = 2, p_l = p_0 = 0, U_{HS} = 1, m = 5$

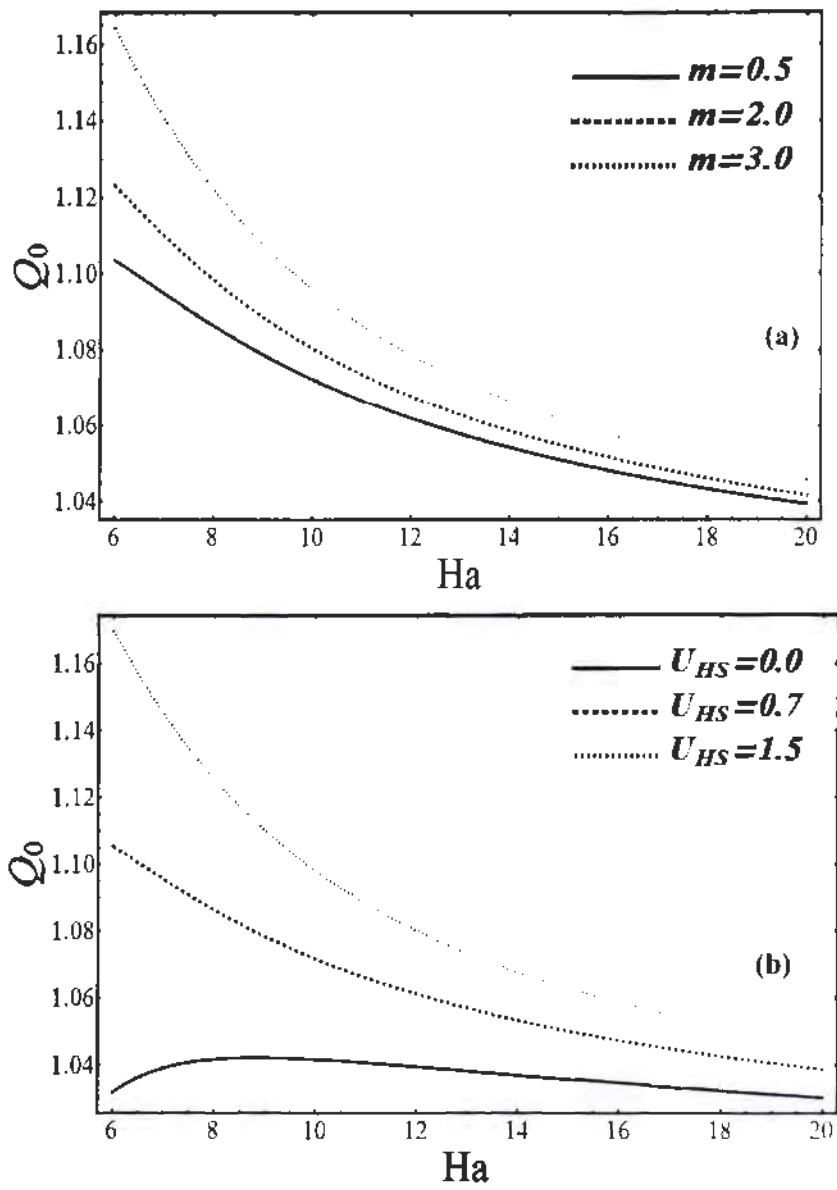


Fig.2.5 Time averaged flow rate (a) $U_{HS} = 1$, for the different Debye length

(b) $m = 5$ for the external electric field. When $\varphi = 0.5$,

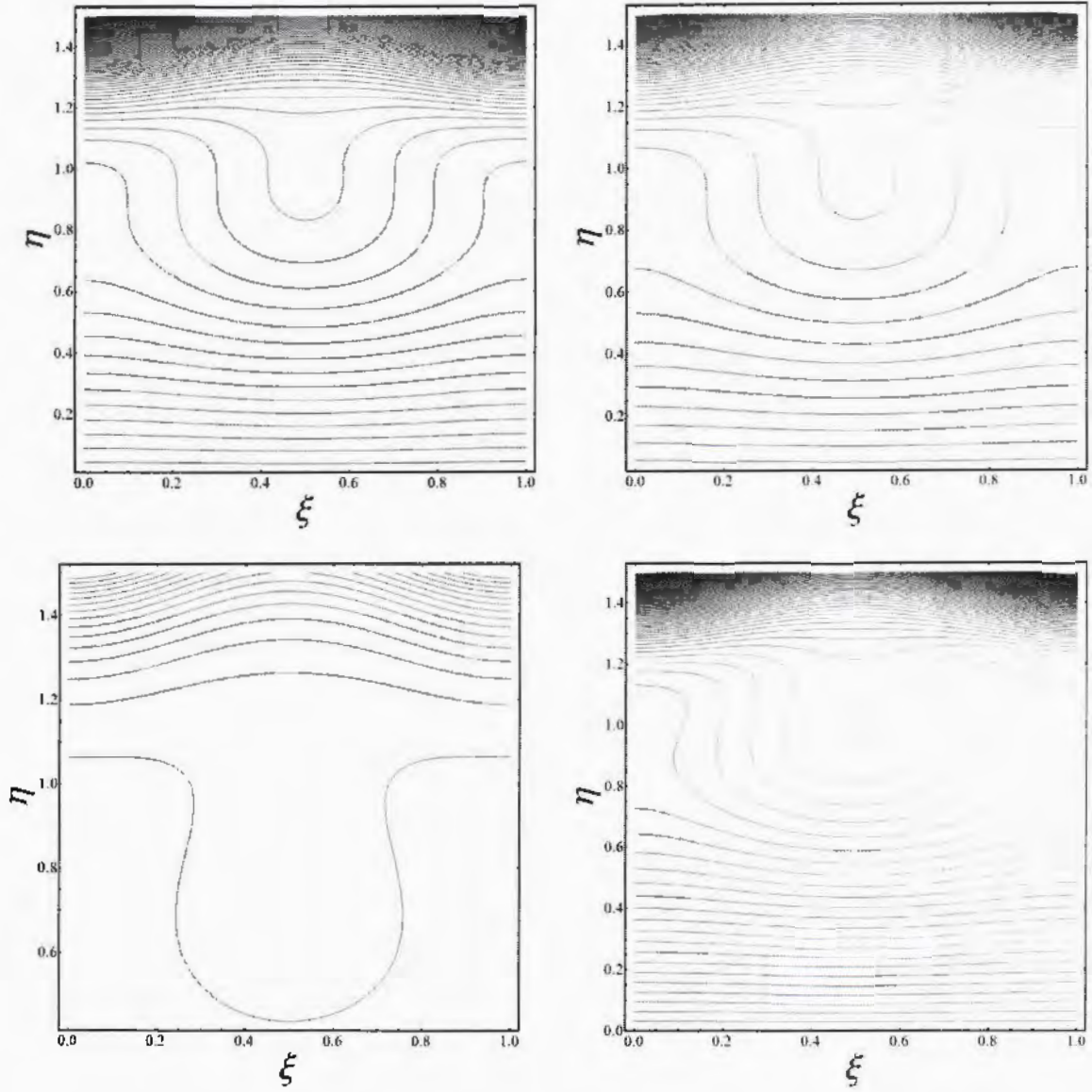


Fig.2.6 Stream lines at (a) $Ha=0.001$, (b) $Ha=2$, (c) $Ha=3$, (d) $Ha=4$.

When $\varphi = 0.6, Q_0 = 0.6, U_{HS} = 1, m = 5$

2.4 Concluding remarks:

Analytical solution has been derived from the un-steady peristaltic transport of Newtonian electrically conducting fluid in the micro channel below the equally perpendicularly applied external magnetic and the electric field under the low Reynolds number and the long wavelength. The electro kinetics derived from the Debye linearization. The solution derived using magneto hydrodynamics and electro kinetics in the biomimetic micro-pumps for the medical presentations. The current computation has been shown:

- By increase the values of Hartmann number, the creation for the bolus in this system is inhibited upon the critical value of the magnetic field. Flow rate reduce with larger Hartmann number as magnitude of the axial velocity and the local wall shear stress. Pressure diff. can establish by increasing the Hartmann number on the low time values, while it reduce by the greater time.
- By raising the electro-osmotic parameter, max averaged flow rate improved, while there is a decrease in axial flow.
- By increasing the electrical field parameter, max averaged flow rate is significantly high.
- By increasing in the axial distance, the pressure differences significantly decrease.

Chapter 3

Electro magneto-hydrodynamic peristaltic transport of dusty fluid

In this chapter, effects of dust particle in peristaltic motion of the dusty fluid through a channel of finite length channel (L). The governing flow problem for the fluid phase and dusty phase is formulated by using then Continuity and Navier-Stokes equations. The resulting partial differential equations have been reduced using long wavelength and creeping flow assumption offer non dimensional equation and solved analytically. The effect of all the physical parameters are drawn for velocity of fluid phase, velocity of particulate phase and pressure difference.

3.1 Mathematical formulation:

The governing equation for the two dimensional, unsteady, electrically conducting and incompressible flow by applying constant magnetic field in transverse direction and electro kinetic body force in axial direction. For fluid and particulate phase in term of Cartesian coordinate system are of the form.

3.1.1 Fluid phase:

$$\frac{\partial U_f}{\partial x} + \frac{\partial V_f}{\partial y} = 0, \quad (3.1)$$

$$(1-C)\rho_f \left\{ \frac{\partial U_f}{\partial t} + U_f \frac{\partial U_f}{\partial x} + V_f \frac{\partial U_f}{\partial y} \right\} = -(1-C) \frac{\partial P}{\partial x} + (1-C)\mu_s \left(\frac{\partial^2 U_f}{\partial x^2} + \frac{\partial^2 U_f}{\partial y^2} \right) + CS(U_p - U_f) + \bar{\rho}_e E_x + \vec{J} \times \vec{B}, \quad (3.2)$$

$$(1-C)\rho_f \left\{ \frac{\partial V_f}{\partial t} + U_f \frac{\partial V_f}{\partial x} + V_f \frac{\partial V_f}{\partial y} \right\} = -(1-C) \frac{\partial P}{\partial y} + (1-C)\mu_s \left(\frac{\partial^2 V_f}{\partial x^2} + \frac{\partial^2 V_f}{\partial y^2} \right) + \bar{\rho}_e E_y + CS(V_p - V_f), \quad (3.3)$$

3.1.2 Particulate phase:

$$\frac{\partial U_p}{\partial x} + \frac{\partial V_p}{\partial y} = 0, \quad (3.4)$$

$$C\rho_p \left\{ \frac{\partial U_p}{\partial t} + U_p \frac{\partial U_p}{\partial x} + V_p \frac{\partial U_p}{\partial y} \right\} = -C \frac{\partial P}{\partial x} + CS(U_f - U_p), \quad (3.5)$$

$$C\rho_p \left\{ \frac{\partial V_p}{\partial t} + U_p \frac{\partial V_p}{\partial x} + V_p \frac{\partial V_p}{\partial y} \right\} = -C \frac{\partial P}{\partial y} + CS(V_f - V_p). \quad (3.6)$$

Using non-dimensional parameter in eq. (2.8) and

$$\xi = \frac{x}{\lambda}, \quad \eta = \frac{y}{a}, \quad u_{f,p} = \frac{U_{f,p}}{c}, \quad v_{f,p} = \frac{V_{f,p}}{c\delta}, \quad (3.7)$$

$$P = \frac{pc\lambda}{a^2} p, \quad \delta = \frac{a}{\lambda}, \quad M_1 = \frac{a^2 SC}{\mu_s}$$

using the equations (3.7), in equations (3.1-3.6), and taking the approximation of low Reynolds number and long wavelength after some simplification we get the resulting equation of fluid phase as:

$$\frac{\partial p}{\partial \xi} = \frac{\partial^2 u_f}{\partial \eta^2} - \frac{m^2}{1-C} U_{HS} \phi + \frac{M_1}{1-C} (u_p - u_f) - \frac{Ha^2}{1-C} u_f, \quad (3.8)$$

$$\frac{\partial p}{\partial \eta} = 0. \quad (3.9)$$

And for Particulate Phase:

$$\frac{\partial p}{\partial \xi} = \frac{M_1}{C} (u_f - u_p), \quad (3.10)$$

$$\frac{\partial p}{\partial \eta} = 0. \quad (3.11)$$

The Second order slip conditions are:

$$\begin{aligned} \frac{\partial u_f}{\partial \eta} &= 0 && \text{at } \eta = 0, \\ u_f &= A \frac{\partial u_f}{\partial \eta} + B \frac{\partial^2 u_f}{\partial \eta^2} && \text{at } \eta = h, \end{aligned} \quad (3.12)$$

$$\text{where } A = \frac{2}{3} \left(\frac{3 - \alpha l^3}{\alpha} - \frac{3(1-l^2)}{2k_n} \right) \text{ and } B = -\frac{1}{4} \left(l^4 + \frac{2(1-l^2)}{k_n^2} \right) \frac{\lambda}{a^2}.$$

3.2 Solution of the problem:

By using equation (3.12) in equations (3.8) and (3.10), we get the equations of fluid and dust phase given below:

$$u_f = C_1 \text{Cosh} \frac{Ha\eta}{\sqrt{1-C}} + C_2 \text{Sinh} \frac{Ha\eta}{\sqrt{1-C}} - \frac{(1-C)}{Ha^2} \left(1 - \frac{C}{1-C} \right) \frac{\partial p}{\partial \xi} - \frac{(1-C)m^2 U_{HS}}{m^2(1-C) - Ha^2} \phi \quad (3.13)$$

$$u_p = C_1 \text{Cosh} \frac{Ha\eta}{\sqrt{1-C}} + C_2 \text{Sinh} \frac{Ha\eta}{\sqrt{1-C}} - \frac{(1-C)}{Ha^2} \left(1 - \frac{C}{1-C}\right) \frac{\partial p}{\partial \xi} - \frac{(1-C)m^2 U_{HS}}{m^2(1-C) - Ha^2} \phi - \frac{C}{M_1} \frac{\partial p}{\partial \xi} \quad (3.14)$$

where,

$$C_1 = \frac{-\frac{(1-C)(1-\frac{C}{1-C})P}{Ha^2} - \frac{(1-C)m^2 U_{HS}}{-Ha^2 + (1-C)m^2} + \frac{B(1-C)m^4 U_{HS}}{-Ha^2 + (1-C)m^2} + \frac{A(1-C)m^3 U_{HS} \text{Tan}[hm]}{-Ha^2 + (1-C)m^2}}{-\text{Cosh}\left[\frac{hHa}{\sqrt{1-C}}\right] + \frac{BHa^2 \text{Cosh}\left[\frac{hHa}{\sqrt{1-C}}\right]}{1-C} + \frac{AHa \text{Sinh}\left[\frac{hHa}{\sqrt{1-C}}\right]}{\sqrt{1-C}}}$$

$$C_2 = 0$$

3.3 Numerical results and discussion:

In this section analytical solution is drawn through graphically. The solution of velocity, pressure, streamlines for fluid and particulate phase are elaborated graphically through various pertinent parameters like Hartmann number (Ha), particle effect (C) and Electro-osmotic parameter (m) having two dimensions having MHD and second order slip condition. The computational software mathematica has been used to visualize the performance of all the parameters through graph.

TH/18/992

3.3.1 Fluid and Particle velocity profile

Figs. (3.1-3.3) represents the behavior of velocity profiles of fluid phase and Figs. (3.4-3.6) represents the behavior of velocity profiles particle phase along the different parameters with the variations of time. From Fig. (3.1) it can be observed that velocity profile of fluid phase shows the relation between velocity and particle effect (C), graphs shows that velocity of fluid phase

decreases with the variations of particle effect (C) due to resistive drag force which is induced due to the presence of particles, whereas velocity profile of particulate phase shows opposite behavior as seen in Fig. (3.4). It is observed that in Fig. (3.2) of velocity profile of fluid phase increase in Hartmann number (Ha) in result decrease in velocity profile graph due to the influence of Lorentz force which resists the flow. In Fig. (3.5) velocity profile of particulate phase shows opposite result. In Fig. 3.3 increase in electro-osmotic parameter (m) decrease in velocity profile graph. The parameter (m) is inversely proportional to Debye length ($\lambda_d = \frac{I}{m}$). It can be seen in Fig. (3.6) velocity profile of particulate phase shows opposite result. All the variations in graphs at different time are remain same.

3.3.2 Pressure gradient

Figs. (3.7-3.9) represents the influence of pressure gradient for different parameters with the variations of time. It can be observed from Fig. 3.7 that the relation between velocity and particle effect (C), by increase the values of particle effect (C) pressure graph increases. Similarly, it can be noted in Fig. 3.8-3.9, increase in Hartmann number (Ha) and electro-osmotic parameter (m), in result increase in pressure graphs respectively.

3.3.3 Skin friction

Figs. (3.10-3.11) represents the role of skin friction with the variations of Hartmann number (Ha) along the different values of particle effect (C) and Electro-osmotic parameter (m) respectively. From Fig. 3.10 it can be noted that by increasing the values of both particle effect (C)

and Hartmann number (Ha), graph gradually increases. Graph of skin friction at different values of particle effect (C) starts from same point and shows same behavior. Similarly, in Fig.3.11. by increasing the value of electro-osmotic (m), graph gradually increase and Hartmann number (Ha) also increase. Skin friction graphs at different values of electro-osmotic (m) starts from different point but shows same trend.

3.3.4 Stream lines

Figs. (3.12 a-d) shows the behavior of streamlines by using the different values of Hartmann number (Ha) along with the fixed set of other parameters. Closed streamlines circulating bolus (defined as a volume of fluid bounded by a closed streamlines) of fluid is formed. In Fig. (3.12 a-d), the trapped bolus is appear when Hartmann number (Ha) is small. It is observed that by increasing the value of Hartmann number (Ha) the trapped bolus start expanding.

The graph of u_f and u_p at different value of time. With the variation of Particle, Hartmann number and electro-osmotic parameter are shown below:

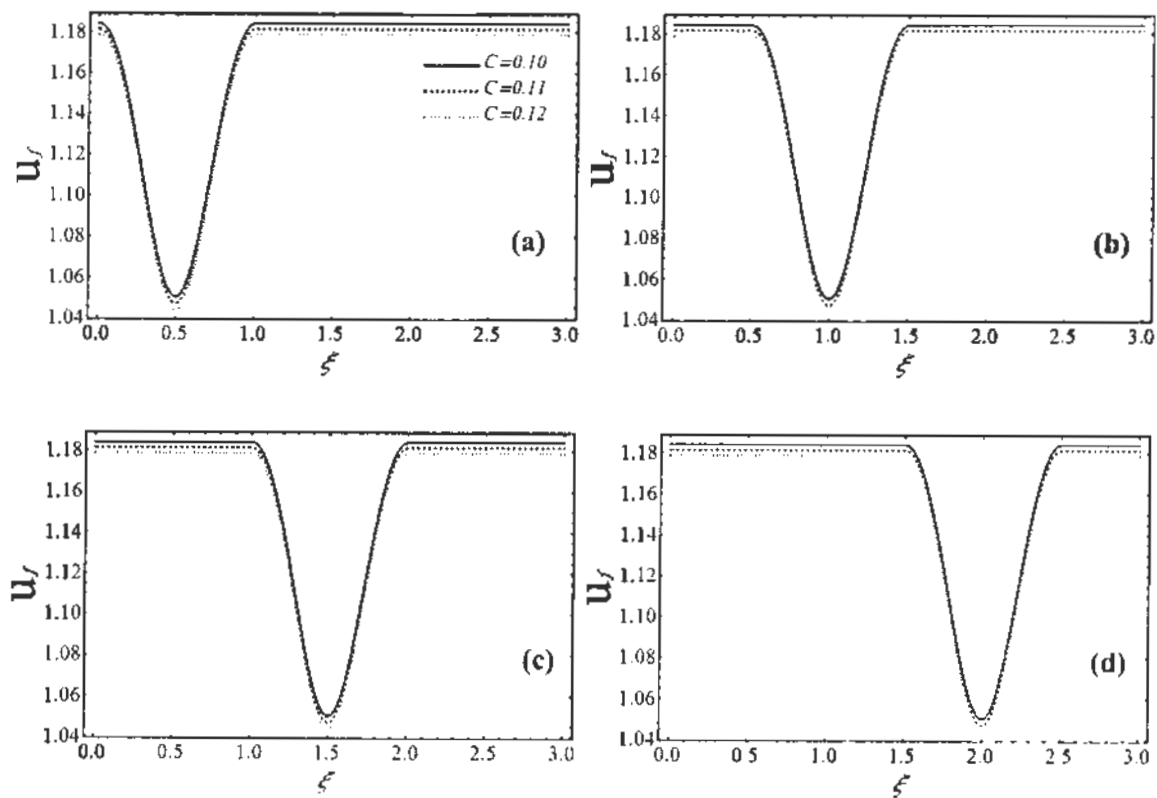


Fig. 3.1 velocity graph for fluid phase at various values of C at

(a) $t = 0$, (b) $t = 0.5$, (c) $t = 1.0$, (d) $t = 1.5$ when $\varphi = 0.6, U_{HS} = 0.1, m = 5$

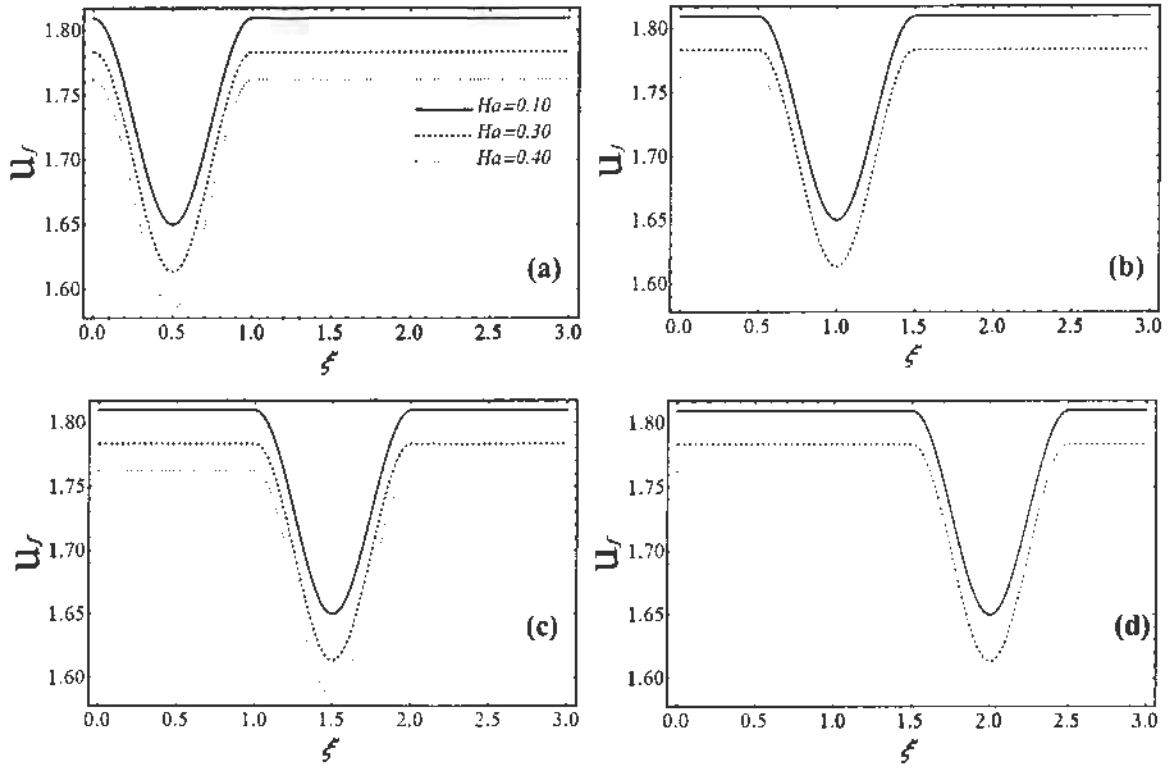


Fig. 3.2 velocity graph for fluid phase at various values of Ha at

(a) $t = 0$, (b) $t = 0.5$, (c) $t = 1.0$, (d) $t = 1.5$ when $\varphi = 0.6, U_{HS} = 0.1, m = 5$

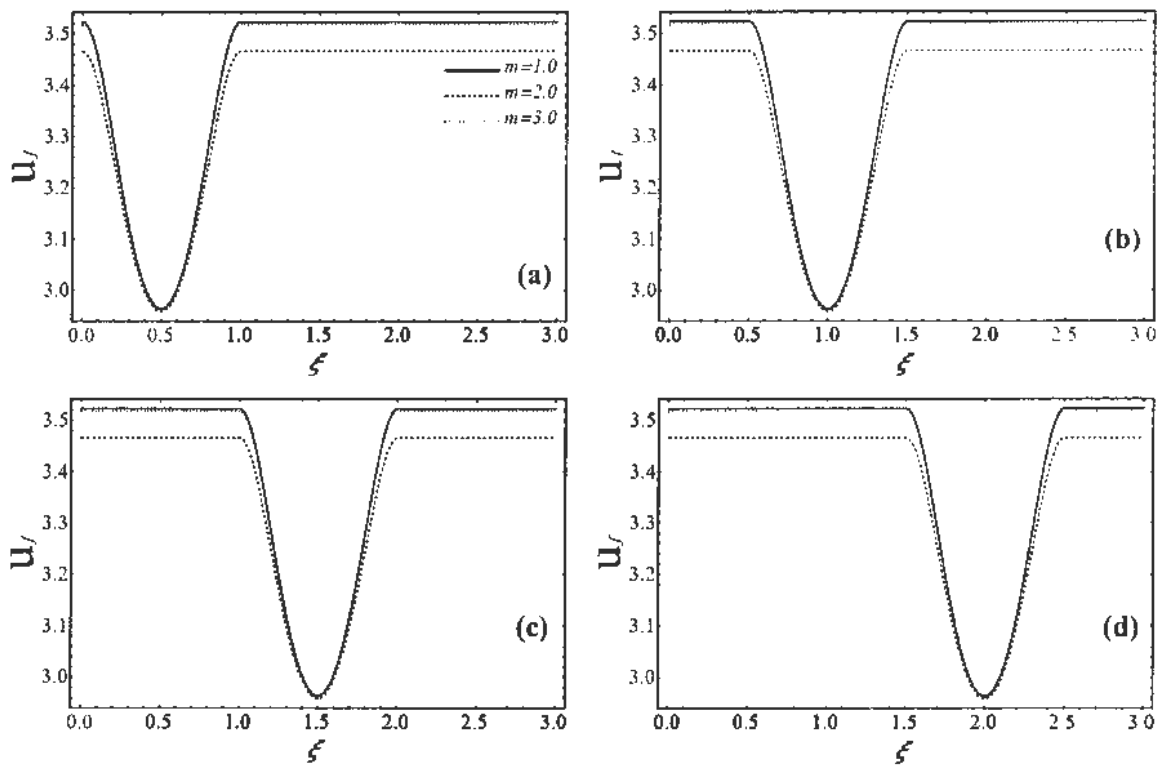


Fig. 3.3 velocity graph for fluid phase at various values of m at

(a) $t = 0$, (b) $t = 0.5$, (c) $t = 1.0$, (d) $t = 1.5$ when

$$\varphi = 0.6, U_{HS} = 0.1, C = 0.1$$

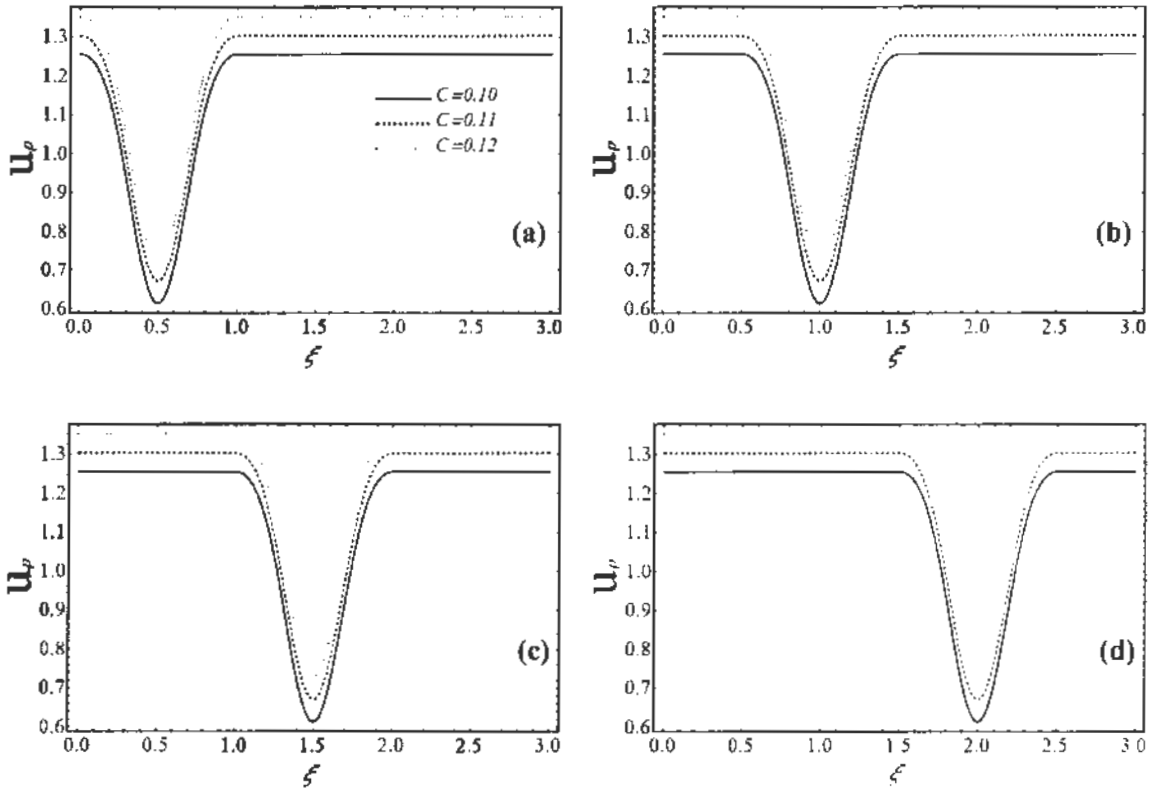


Fig. 3.4 velocity graph for particulate phase at various values of C at

(a) $t=0$, (b) $t=0.5$, (c) $t=1.0$, (d) $t=1.5$ when $\varphi=0.6, U_{HS}=0.1, m=5$

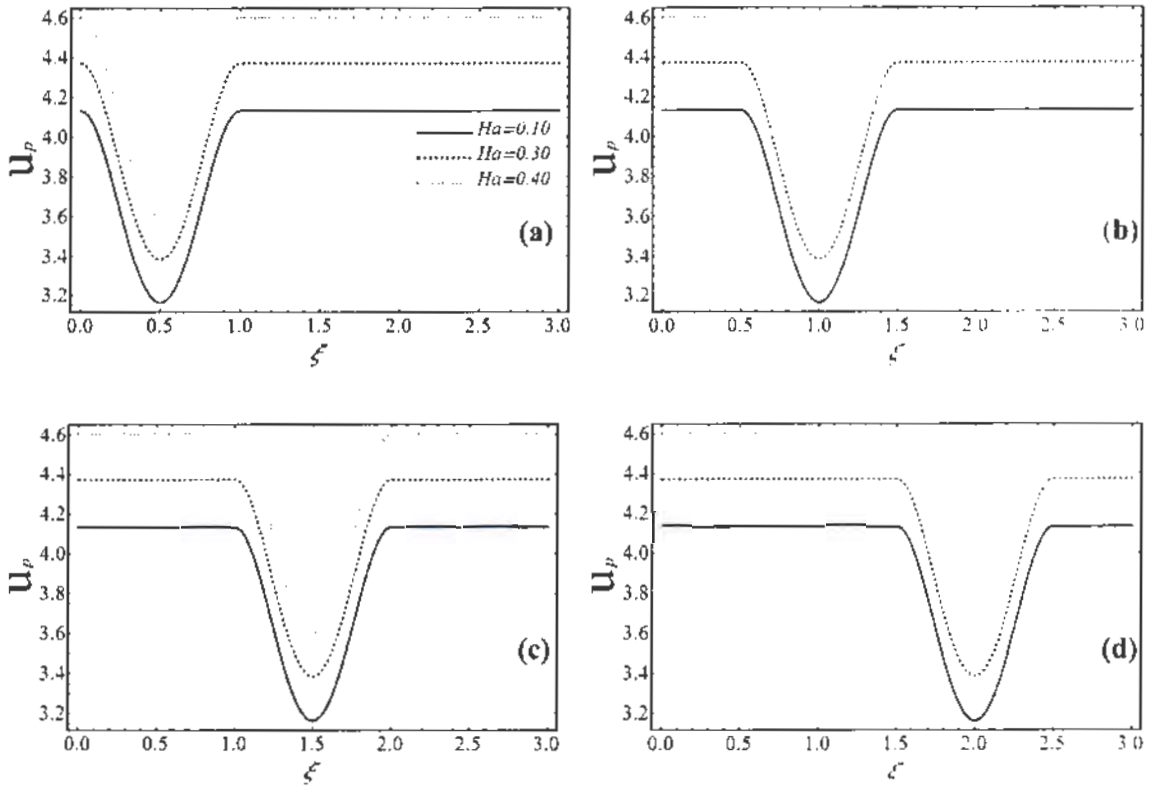


Fig. 3.5 velocity graph for particulate phase at various values of Ha at

(a) $t=0$, (b) $t=0.5$, (c) $t=1.0$, (d) $t=1.5$ when $\varphi=0.6, U_{HS}=0.1, m=5$

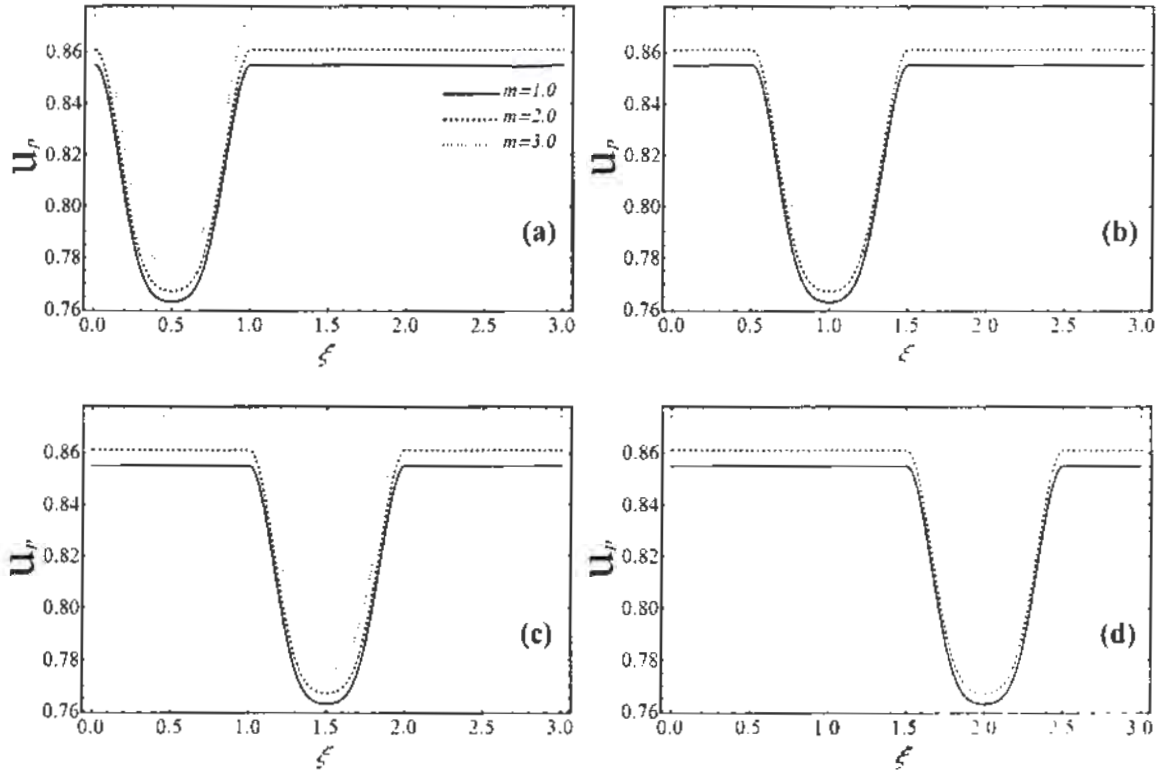


Fig. 3.6 velocity graph for particulate phase at various values of m at

(a) $t = 0$, (b) $t = 0.5$, (c) $t = 1.0$, (d) $t = 1.5$ when

$$\varphi = 0.6, U_{HS} = 0.1, C = 0.1$$

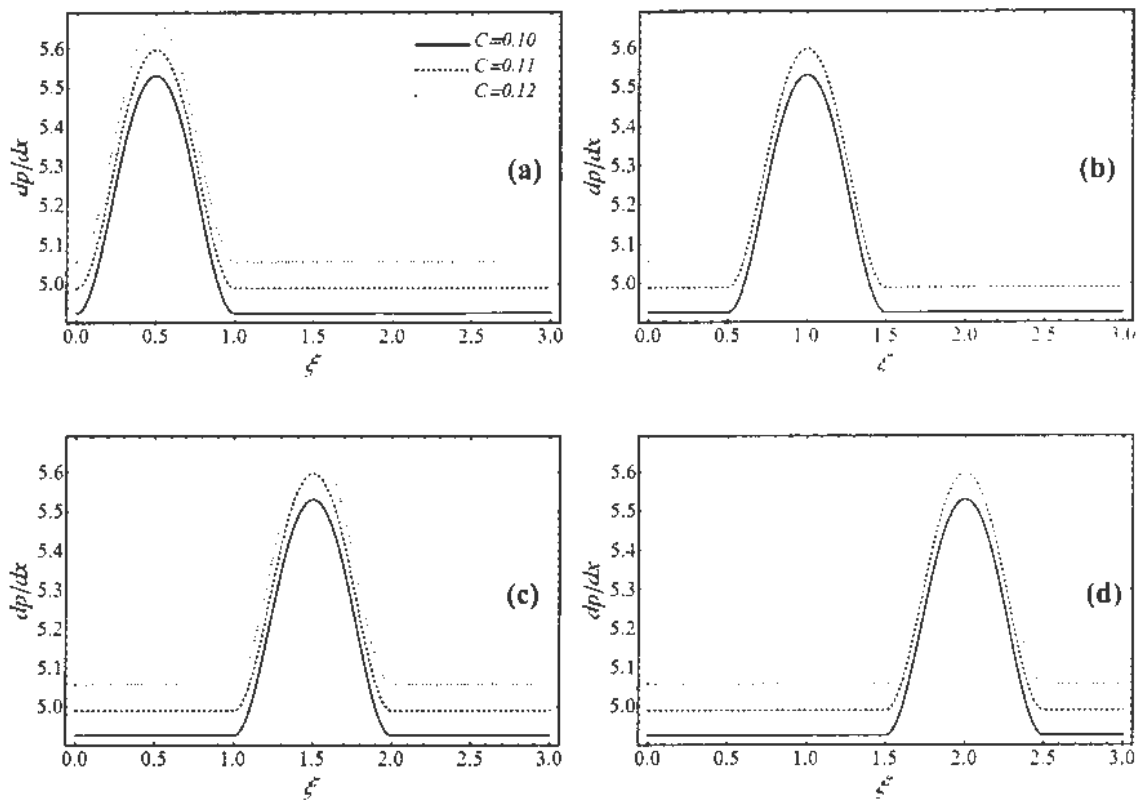


Fig. 3.7 Pressure gradient at various values of C at

(a) $t = 0$, (b) $t = 0.5$, (c) $t = 1.0$, (d) $t = 1.5$ when $\varphi = 0.6, U_{HS} = 0.1, m = 5$

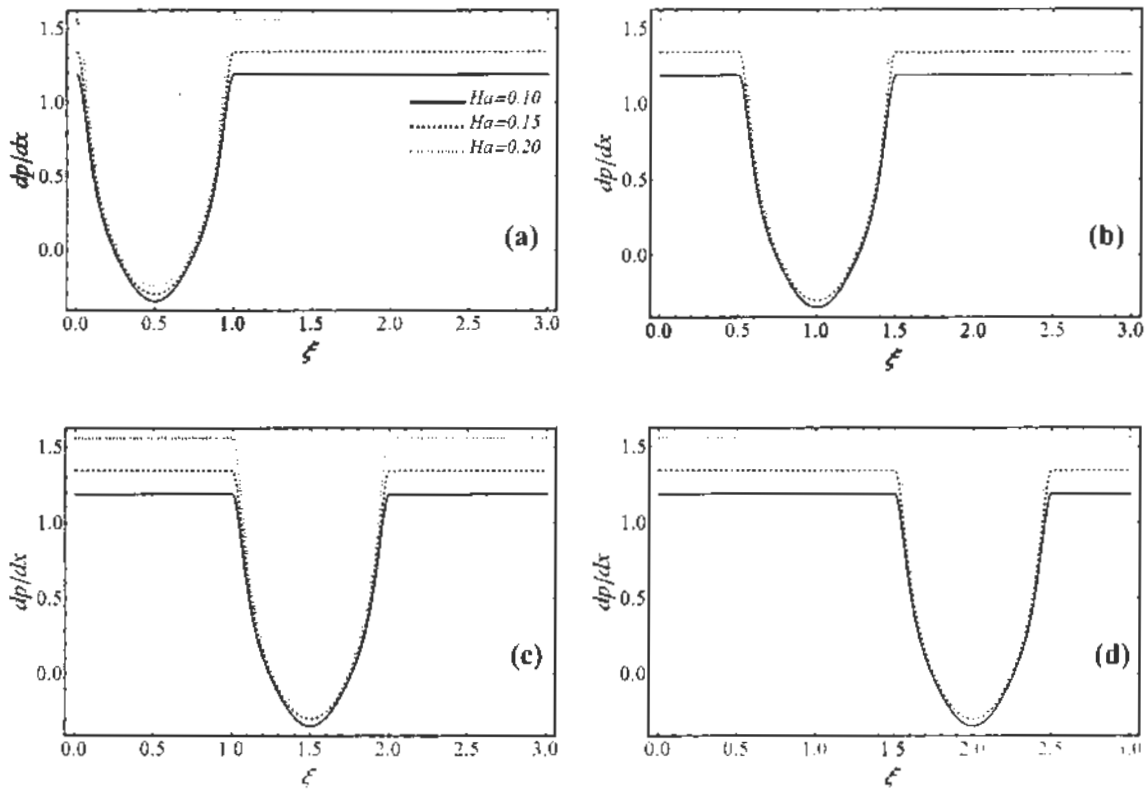


Fig. 3.8 Pressure gradient at various values of Ha at

(a) $t = 0$, (b) $t = 0.5$, (c) $t = 1.0$, (d) $t = 1.5$ when

$$\varphi = 0.6, U_{HS} = 0.1, C = 0.1$$

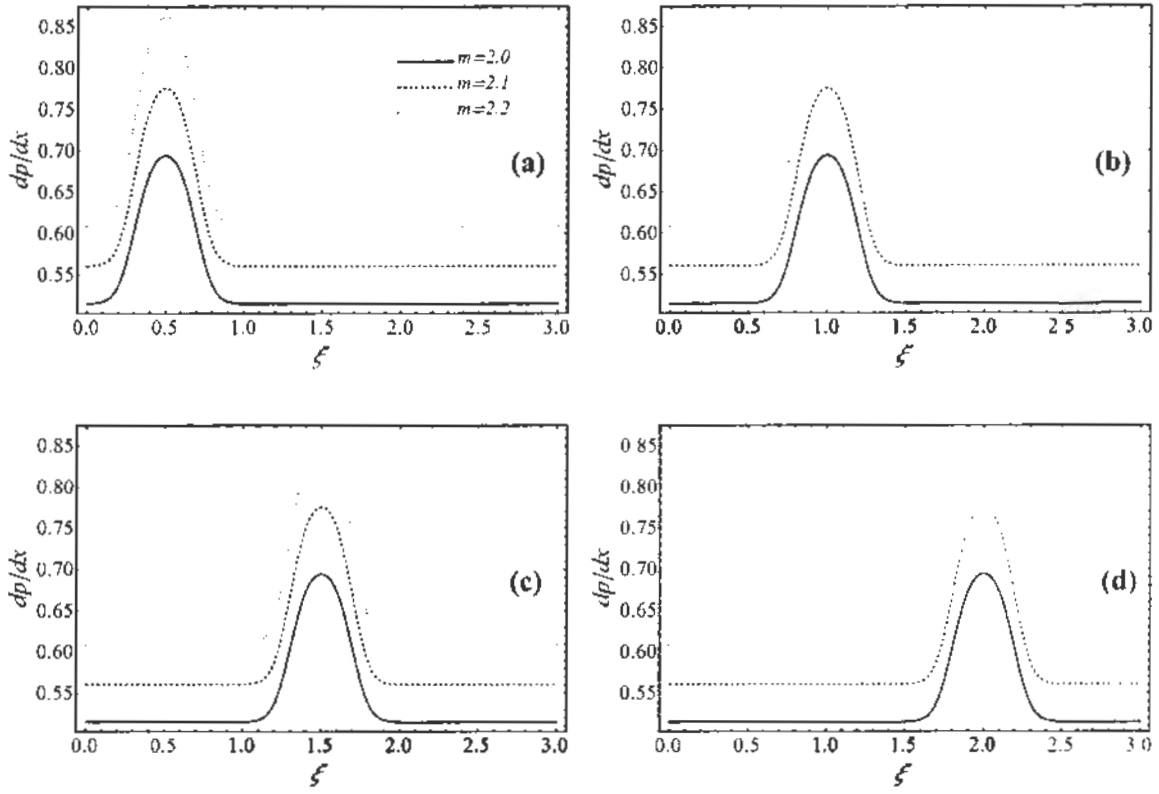


Fig. 3.9 Pressure gradient at various values of m at

(a) $t = 0$, (b) $t = 0.5$, (c) $t = 1.0$, (d) $t = 1.5$ when

$$\varphi = 0.6, U_{HS} = 0.1, C = 0.1$$

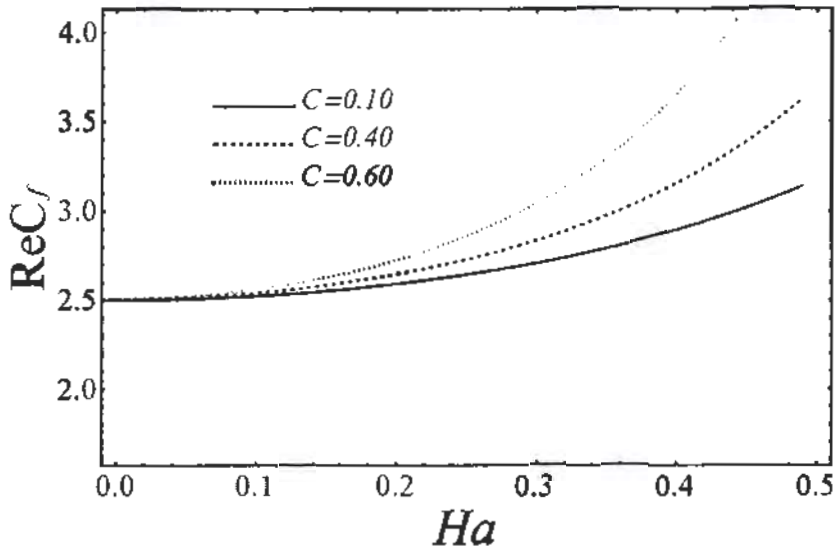


Fig. 3.10 Skin friction at various values of C , when

$$\varphi = 0.6, U_{HS} = 1, m = 5$$

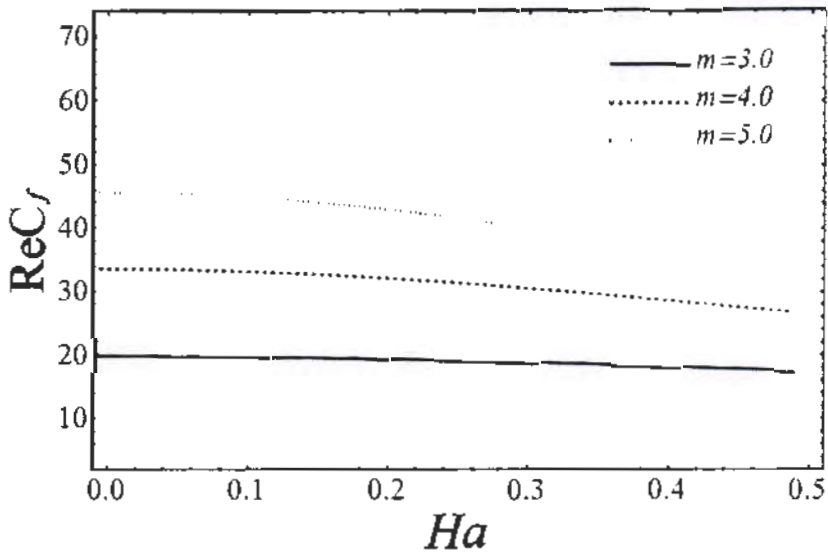


Fig. 3.11 Skin friction at various values of m , when

$$\varphi = 0.6, U_{HS} = 1, C = 0.1$$

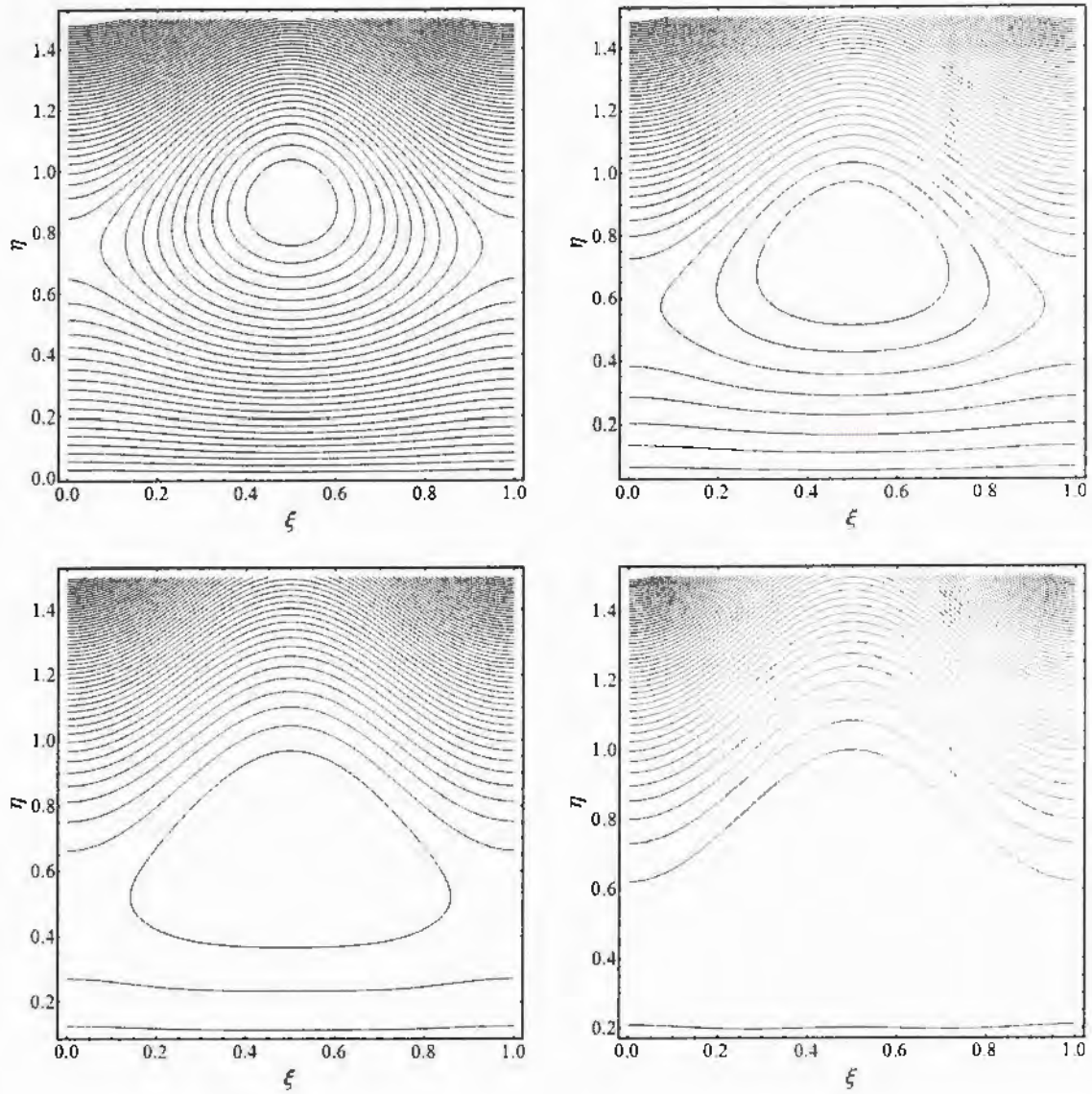


Fig. 3.12 stream lines w.r.t u_f at various values of Ha , when

$$\varphi = 0.6, U_{HS} = 1, m = 5, C = 0.1$$

3.4 Concluding remarks:

This chapter discusses MHD peristaltic flow of dusty fluid. This flow is described by the continuity and Navier-Stokes equations. This fluid is assumed to be unsteady, electrically-conducting, and incompressible. Under the assumptions of long wave length and low Reynolds number, the governing equations of fluid and particulate equations are solved. The solution is obtained numerically. The effects of the Hartmann number (Ha), Particle effect (C), and Electro-osmotic parameter (m) are studied. The major outcomes of our current examination are summarized below:

- From the above mathematical analysis, it can be seen that by increasing the Hartmann number (Ha), Particle effect (C), and Electro-osmotic parameter (m) fluid velocity decreases, while particulate velocity increases.
- It can be seen from graphs, pressure gradient graphs increase by increasing the values of Hartmann number (Ha), Particle effect (C), and Electro-osmotic parameter (m) parameters.
- There is no effect on the graphs even the variation of time. All graphs show the same result at different times.
- In the streamlines, by increasing the Hartmann number trapped bolus starts expanding.
- In skin friction, by increasing the particle effect and electro-osmotic parameter, skin friction increases.

References

- [1] D. Tripathi and O. Anwar Bég, Transverse Magnetic Field Driven Modification in Unsteady Peristaltic Transport with Electrical Double Layer Effects, *Colloids and Surfaces A: Physicochemical and Engineering Aspects*, COLSUA-D-16-00391.
- [2] B.D. Iverson, S.V. Garimella, Recent advances in microscale pumping technologies: a review and evaluation, *Microfluid Nanofluid* (2008) 5: 145–174.
- [3] K.E. Goodson et al. Electro-osmotic microchannel cooling system, U.S. Patent 6,942,018, issued September 13 (2005).
- [4] J. Xie, J. Shih, Q. Lin, B. Yang and Y-C. Tai, Surface micro-machined electrostatically actuated micro peristaltic pump, *Lab Chip*, (2004) 4, 495-501.
- [5] T. Brettschneider and C. Dorrer, Microfluidic peristaltic pump, method and pumping system, U.S. Patent Application, 14/075,301 (2013).
- [6] H.P. Chou, A.Y. Fu and S. R. Quake, Microfluidic devices and methods of use, U.S. Patent No.8,992,858. 31 Mar. (2015).
- [7] X. Zhang, Z. Chen and Y. Huang, A valve-less microfluidic peristaltic pumping method, *Biomicrofluidics*, 9, 014118 (2015).
- [8] D. Si and Y. Jian, Electromagnetohydrodynamic (EMHD) micropump of Jeffrey fluids through two parallel microchannels with corrugated walls, *J. Phys. D: Appl. Phys.* 48 (2015) 085501 (10pp)
- [9] J.C. Burns and T. Parkes, Peristaltic motion, *J. Fluid Mechanics*, 29 (1967): 731-743.
- [10] Y.C. Fung and C.S. Yih, Peristaltic transport, *ASME J. Applied Mechanics*, 35 (1968): 669-675.
- [11] A.H. Shapiro, M.Y. Jaffrin and S.L. Weinberg, Peristaltic pumping with long wavelengths at low Reynolds number, *J. Fluid Mechanics*, 37 (1969): 799-825.
- [12] M.Y. Jaffrin and A. H. Shapiro, Peristaltic pumping, *Ann. Rev. Fluid Mechanics*, 3 (1971): 13-37.21
- [13] J.B. Shukla, R. S. Parihar, B. R. P. Rao and S. P. Gupta, Effects of peripheral-layer viscosity on peristaltic transport of a bio-fluid, *J. Fluid Mechanics*, 97 (1980): 225-237.
- [14] S. Takabatake and K. Ayukawa, Numerical study of two-dimensional peristaltic flows, *J. Fluid Mechanics*, 122 (1982): 439-465.
- [15] C. Pozrikidis, A study of peristaltic flow, *J. Fluid Mechanics*, 180 (1987): 515-527.
- [16] M. Li and J.G. Brasseur, Non-steady peristaltic transport in finite-length tubes, *J. Fluid Mechanics*, 248 (1993): 129-151.
- [17] D. Tripathi and O. Anwar Bég, Peristaltic propulsion of generalized Burgers' fluids through a non-uniform porous medium: A study of chyme dynamics through the diseased intestine, *Mathematical Biosciences*, 248 (2014): 67-77.
- [18] D. Tripathi and O. Anwar Bég, Transient magneto-peristaltic flow of couple stress biofluids: a magneto-hydro-dynamical study on digestive transport phenomena, *Mathematical Biosciences*, 246.1(2013): 72-83.
- [19] F. Blanchette, The influence of suspended drops on peristaltic pumping, *Phys. Fluids* 26.6 (2014): 061902.

- [20] R. Ellahi, M. Mubashir Bhatti, and K. Vafai, Effects of heat and mass transfer on peristaltic flow in a non-uniform rectangular duct, *Int. J. Heat Mass Transfer*, 71 (2014): 706-719.
- [21] D. Tripathi and O. Anwar Bég, A study on peristaltic flow of nanofluids: Application in drug delivery systems, *Int. J. Heat Mass Transfer*, 70 (2014): 61-70.